Semirubin. A Novel Dipyrrinone Strapped by Intramolecular Hydrogen Bonds

Michael T. Huggins and David A. Lightner*

Department of Chemistry, University of Nevada, Reno, Nevada 89557-0020

lightner@scs.unr.edu

Received March 17, 2000

(4*Z*)-9-(5-Carboxypentyl)-2,3,7,8-tetramethyl-(10*H*)-dipyrrin-1-one (**1**, semirubin), a new dipyrrinone model for one-half of bilirubin, the yellow-orange neurotoxic pigment of jaundice, was synthesized following Friedel−Crafts acylation of 2,3,7,8-tetramethyl-(10*H*)-dipyrrin-1-one (**5**) with the half-ester acid chloride of adipic acid. Unlike other dipyrrinone models for bilirubin, such as the xanthobilirubic acids, which engage only in *inter*molecular hydrogen bonding, **1** is unique in having been designed and found to engage in *intra*molecular hydrogen bonding, between the carboxylic acid and the dipyrrinone lactam and pyrrole. This important conformation-determining structural characteristic, shared by **1** and bilirubin, renders them less polar than their methyl esters and leaves them monomeric in nonpolar solvents, where their esters are dimeric. The corresponding 10-oxo analogue (**3**) of **1** serves as a model for 10-oxo-bilirubin, a presumed bilirubin metabolite in alternate pathways for bilirubin excretion. Like **1**, **3** is found to engage in intramolecular hydrogen bonding. Unlike the methyl ester of **1**, the ethyl ester of **3** is not intermolecularly hydrogen bonded in nonpolar solvents.

Introduction

Bilirubin (Figure 1), the end product of heme metabolism in mammals and the festuscine pigment of jaundice,[1] is comprised of two dipyrrinone chromophores, each with a single propionic acid. The dipyrrinones are conjoined at and capable of independent rotations about a central CH_2 group. Such rotations bring the propionic carboxyl group on one dipyrrinone into sufficiently close proximity to engage the opposing dipyrrinone's lactam and pyrrole moieties in intramolecular hydrogen bonding (Figure 1, middle). Taken collectively, these (six) intramolecular hydrogen bonds are potent stabilizers of a unique conformation, shaped like a ridge-tile, and they thereby control the solution, spectroscopic, and metabolic properties of bilirubin.[2−4]

Structurally simpler dipyrrinone models for half of bilirubin, such as xanthobilirubic acid (Figure 1, bottom) have been important in understanding the chemistry and photobiology of bilirubin. Although many dipyrrinones are now known, among the earliest were the xanthobilirubic acids, prepared long ago by Fischer following treatment of bilirubin dimethyl ester with molten resorcinol.[5] Fischer and others subsequently prepared various xanthobilirubic acids by rational synthesis.[6] Typical dipyrrinones are bright yellow compounds with an intense UV−visible absorption ($\epsilon^{max} \sim 30\,000$ L mol^{-1} cm^{-1}) near 400 nm associated with a long-axis-polarized $\pi \rightarrow \pi^*$ excitation of the 14π electron conjugated chromophore (Figure 1).[4] They are known from X-ray crystallography,[4,7] NMR spectroscopy[4] and molecular mechanics calculations[2,4,8] to prefer the lactam tautomer and the *Z*-configuration at C(4). Whether in bilirubin or in xanthobilirubic acid and its analogues, dipyrrinones are avid participants in hydrogen bonding.[4,9,10] Individual dipyrrinones adopt essentially planar conformations (torsion angle C(4)−C(5)−C(6)−N ∼0°) in the crystal, where they are present as intermolecularly hydrogen-bonded planar dimers (Figure 2)[4,7] that persist in solutions of nonpolar solvents. In $CHCl_3$, for example, methyl xanthobilirubinate is strongly self-associated with dimers conglutinated by four hydrogen bonds and a dimerization constant of ∼25 000 M^{-1} (22 °C), as measured by ^{1}H NMR

(1) (a) Chowdhury, J. R.; Wolkoff, A. W.; Chowdhury, N. R.; Arias, I. M. Hereditary Jaundice and Disorders of Bilirubin Metabolism. In *The Metabolic and Molecular Bases of Inherited Disease*; Scriver, C. R., Beaudet, A. L., Sly, W. S., Valle, D., Eds.; McGraw-Hill: New York, 1995; Vol. 2, Chapter 67, pp 2161−2208. (b) Berk, P. D.; Noyer, C. *Seminars Liver Dis.* **1994**, *14*, 323−394. (c) McDonagh, A. F. Bile Pigments: Bilatrienes and 5, 15-Biladienes. In *The Porphyrins*; Dolphin, D., Ed., Academic Press: New York, 1979; Vol. 6, 293−491.

(2) Person, R. V.; Peterson, B. R.; Lightner, D. A. *J. Am. Chem. Soc.* **1994**, *116*, 42−59.

(3) (a) Lightner, D. A.; McDonagh, A. F. *Acc. Chem. Res.* **1984**, *17*, 417−424. (b) McDonagh, A. F.; Lightner, D. A. *Pediatrics* **1985**, *75*, 443−455. (c) McDonagh, A. F.; Lightner, D. A. *Seminars in Liver Disease* **1988**, *8*, 272−283. (d)McDonagh, A. F.; Lightner, D. A. In *Hepatic Metabolism and Disposition of Endo and Xenobiotics*; Falk Symposium No. 57; Bock, K. W., Gerok, W., Matern, S., Eds.; Kluwer: Dordrecht, The Netherlands, 1991; Chapter 5, pp 47−59. (e) McDonagh, A. F.; Lightner, D. A. *Cell. Mol. Biol.* **1994**, *40*, 965−974.

(4) For leading references, see: Falk, H. *The Chemistry of Linear Oligopyrroles and Bile Pigments*; Springer-Verlag: New York, 1989.

(5) Fischer, H.; Plieninger, H. *Z. Physiol. Chem.* **1941**, *268*, 197−226.

(6) (a) Fischer, H.; Hartmann, P. *Z. Physiol. Chem.* **1934**, *226*, 116−129. (b) Siedel, W.; Fischer, H. *Z. Physiol. Chem.* **1933**, *214*, 145−172. (c) Siedel, W. *Z. Physiol. Chem.* **1935**, *231*, 167−198. (d) Grunewald, J. O.; Cullen, R.; Bredfeldt, J.; Strope, E. R. *Org. Prep. Proc. Intl.* **1975**, *7*, 103−110. (e) Lightner, D. A.; Ma, J.-S.; Adams, T. C.; Franklin, R. W.; Landen, G. L. *J. Heterocycl. Chem.* **1984**, *21*, 139−144. (f) Shrout, D. P.; Lightner, D. A. *Synthesis* **1990**, 1062−1065.

(7) For leading references, see: Sheldrick, W. S. *Isr. J. Chem.* **1983**, *23*, 155−166.

(8) Falk, H.; Müller, N. *Tetrahedron* **1983**, *39*, 1875−1885.

(9) Nogales, D. F.; Ma, J.-S.; Lightner, D. A. *Tetrahedron* **1993**, *49*, 2361−2372.

(10) (a) Boiadjiev, S. E.; Anstine, D. T.; Lightner, D. A. *J. Am. Chem. Soc.* **1995**, *117*, 8727−8736. (b) Boiadjiev, S. E.; Anstine, D. T.; Maverick, E.; Lightner, D. A. *Tetrahedron: Asymmetry* **1995**, *6*, 2253−2270.

10.1021/jo000393k CCC: $19.00
Published on Web 08/30/2000

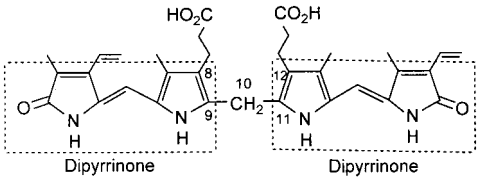

Bilirubin

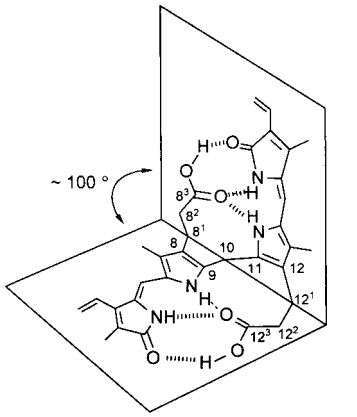

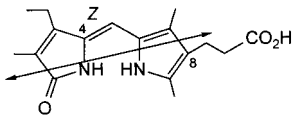

Xanthobilirubic Acid

Figure 1. (Top) Bilirubin, shown in the conformationally unstable linear representation, is composed of two dipyrrinone chromophores. (Middle) The most stable bilirubin conformation, shaped like a ridge-tile with hydrogen bonds shown by dashed lines between the carboxylic acid groups and the opposing dipyrrinones. (Bottom) A typical dipyrrinone, (4*Z*)-xanthobilirubic acid. The double-headed arrow approximates the long axis polarization of the intense ~400 nm electronic transition of the dipyrrinone chromophore.

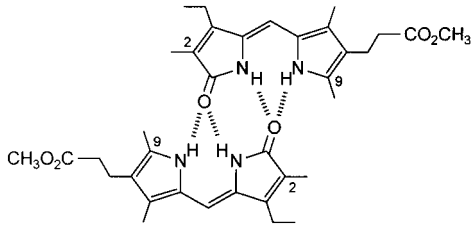

Methyl Xanthobilirubinate
Planar Dimer

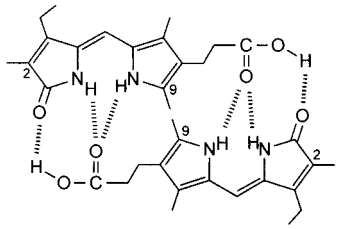

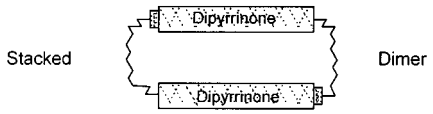

Figure 2. Dipyrrinone dimers. (Top) Most stable dimer of methyl xanthobilirubinate and related dipyrrinones with four intermolecular hydrogen bonds. Consistent with this dimeric representation, ^{1}H NMR NOEs measured in $CDCl_3$ are found between the methyls at C(2) and C(9) (ref 8). (Middle) Favored dimer in xanthobilirubic acid, with six intermolecular hydrogen bonds, as in bilirubin. (Bottom) Schematic representation for the shape of most stable dimer of xanthobilirubic acid. The dipyrrinones are stacked, thereby alleviating a nonbonded steric repulsion between the methyls at C(9).

spectroscopy.[9] The coplanar dipyrrinone-to-dipyrrinone motif (Figure 2, top) is probably the most common type of hydrogen-bonding in dipyrrinone dimers[4,10] (and is found even in bilirubin dimethyl ester[4,11a,12]); however, when a carboxylic acid group is present (as in xanthobilirubic acid) another type of hydrogen bonded dimer may become more stable (Figure 2, middle) by using the rare carboxylic acid to amide hydrogen bonding motif.[13] Thus, dipyrrinone acids, unlike simple C-alkylated dipyrrinones and dipyrrinone esters, may form π-facial stacked dimers in which each carboxylic acid group is engaged in hydrogen bonding to an opposing dipyrrinone, as found in xanthobilirubic acid and its alkanoic acid homologues.[10] Dipyrrinone acids may thus eschew the planar dimer with its four intermolecular hydrogen bonds in favor of gaining the added stabilization due to a total of six hydrogen bonds. This preference of dipyrrinones to hydrogen bond to carboxylic acid groups is not surprising in view of the precedence found in bilirubin, whose planar dipyrrinones are tightly hydrogen bonded, albeit intramolecularly, to neighboring carboxylic acid groups (Figure 1).

Although xanthobilirubic acid has served well as a model compound for bilirubin in many diverse studies,[14] it fails as a true hydrogen-bonded analogue because it is dimeric in nonpolar solvents and its propionic acid is sequestered via *inter*molecular hydrogen bonds to a dipyrrinone.[10] While similar in some ways to the intermolecularly hydrogen-bonded stacked dimer of xanthobilirubic acid, the intramolecular hydrogen bonding pattern in bilirubin is unique, and until recently[15] represented the only well-established example of intramolecular carboxylic acid to amide hydrogen bonding.

(11) (a) Kaplan, D.; Navon, G. *Isr. J. Chem.* **1983**, *23*, 177−186. (b) Kaplan, D.; Navon, G. *Biochem. J.* **1982**, *201*, 605−613. (c) Navon, G.; Frank, S.; Kaplan, D. *J. Chem. Soc., Perkin Trans. 2* **1984**, 1145−1149.

(12) Trull, F. R.; Ma, J. S.; Landen, G. L.; Lightner, D. A. *Isr. J. Chem.* **1983**, *23*, 211−218.

(13) Wash, P. L.; Maverick, E.; Chiefari, J.; Lightner, D. A. *J. Am. Chem. Soc.* **1997**, *119*, 3802−3806.

(14) (a) Grunewald, J. O.; Walker, J. C.; Strope, E. R. *Photochem. Photobiol.* **1975**, *24*, 29−40. (b) Lightner, D. A.; Park, Y.-T. *Tetrahedron Lett.* **1976**, 2209−2212. (c) Lightner, D. A. *Photochem. Photobiol.* **1977**, *26*, 427−436. (d) Lightner, D. A.; Park, Y.-T. *Tetrahedron* **1979**, *35*, 463−471. (e) Matheson, I. B. C.; Lightner, D. A. *Photochem. Photobiol.* **1979**, *29*, 933−935. (f) Lightner, D. A.; Rodgers, S. L. *Experientia* **1981**, *37*, 1245−1246. (g) Lamola, A. A.; Braslavsky, S. E.; Schaffner, K.; Lightner, D. A. *Photochem. Photobiol.* **1983**, *37*, 263−270. (h) Landen, G. L.; Park, Y.-T.; Lightner, D. A. *Tetrahedron* **1983**, *39*, 1893−1907. (i) Lightner, D. A.; Gawroński, J. K.; Gawrońska, K. *J. Am. Chem. Soc.* **1985**, *107*, 2456−2461. (j) Reisinger, M.; Lightner, D. A. *J. Inclusion Phenom.* **1985**, *3*, 479−486. (k) Lightner, D. A.; Reisinger, M.; Landen, G. L. *J. Biol. Chem.* **1986**, *261*, 6034−6038. (l) Lightner, D. A.; Gawroński, J. K.; Wijekoon, W. M. D. *J. Am. Chem. Soc.* **1987**, *109*, 6354−6362. (m) Trull, F. R.; Franklin, R. W.; Lightner, D. A. *J. Heterocycl. Chem.* **1987**, *24*, 1573−1579.

(15) (a) Chen, Q.; Lightner, D. A. *J. Org. Chem.* **1998**, *63*, 2665−2675. (b) Tipton, A. K.; Lightner, D. A. *Monatsh. Chem.* **1999**, *130*, 425−440.

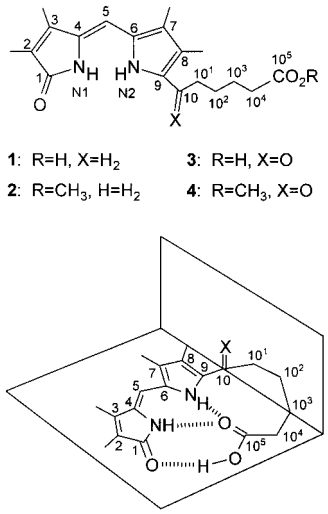

Figure 3. (Top) Semirubin **1**, its methyl ester (**2**), 10-oxo analogue (**3**) and 10-oxo methyl ester (**4**). (Bottom) Intramolecularly hydrogen-bonded conformation of semirubin (**1**, X = H_2) and its 10-oxo analogue (**3**, X = O). Hydrogen bonds are represented by dashed lines. The shape is similar to one-half of bilirubin in Figure 1.

In the simplest analysis, examination of intramolecularly hydrogen-bonded bilirubin (Figure 1) reveals a chain of 6 carbon atoms, attached at C(9) of the dipyrrinone and terminating in a carboxylic acid group, e.g., C(9)−C(10)−C(11)−C(12)−C(12^1)−C(12^2)−C(12^3). In the following, we describe how a simple dipyrrinone tethered to a 6-carbon acid (hexanoic acid) may be constructed and show that it engages in *intra*molecular hydrogen bonding of the type characteristic of bilirubin. We call the new pigment semirubin (**1**, Figure 3). In the course of the synthesis of **1**, we prepared its 10-oxo analogue (**3**), which is also capable of intramolecular hydrogen bonding and serves as a dipyrrinone model for 10-oxo-bilirubin, a proposed metabolite formed in alternate pathways of bilirubin excretion.[16]

Results and Discussion

Synthesis. Armed with knowledge that dipyrrinones can be acylated at unsubstituted α- and *β*-positions of the pyrrole ring,[4,15,17] we envisioned a synthesis of **1** (Scheme 1) that follows from straightforward coupling of 2,3,7,8-tetramethyldipyrrinone (**5**) with the half-ester acid chloride of adipic acid (**6**). *β*-Alkylated dipyrrinones such as **5**[15a,18,19] are relatively easy to prepare, and **6** can be obtained in high yield from adipic acid.[20] Unexpectedly, the reaction conditions that smoothly gave high yields of acylation at a vacant dipyrrinone *β*-position,[17] or benzoylation of a vacant-dipyrrinone α-position,[15a] failed to give satisfactory yields of acylated product **4**. When **5** was reacted with **6** using $SnCl_4$ catalyst, the yield of **4** was only ∼15%. Nevertheless, the acylation showed initial promise, and by adjusting the reaction conditions

Scheme 1[a]

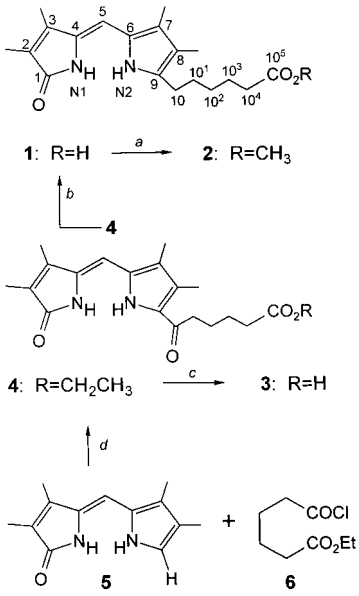

[a] Key: (a) CH_3OH/H_2SO_4, 95%; (b) $NaBH_4/(CH_3)_2CHOH$ refl., 97%; (c) NaOH/THF, 90%; (d) $AlCl_3/CH_2Cl_2$, 64%.

and changing the Lewis acid catalyst to $AlCl_3$, we were able to obtain a 64% isolated yield of **4**. Saponification of **4** gave **3** in 90% yield, and reduction of **4** with $NaBH_4$ proceeded smoothly in refluxing isopropyl alcohol to give **1** in 97% yield. The methyl ester (**2**) could be obtained in 95% yield by Fischer esterification of **1**.

Molecular Structure. The constitutional structures of **1**−**4** (Figure 3, Scheme 1) follow from the structure of the common starting well-known dipyrrinone (**5**)[18,19] and from their syntheses. They were confirmed by their ^{13}C NMR spectra run in $CDCl_3$, and all assignments were made by HMQC and HMBC experiments. Thus, in $CDCl_3$ solvent, **1**−**4** show chemical shifts (Table 1) characteristic of the dipyrrinone unit and the hexanoic acid or 5-carbo(ethoxy)pentanoyl fragment—consistent with the postulated structures. Characteristically, C(8) of **1** and **2** is much more deshielded than C(8) in the parent (**5**) or the oxo analogues (**3** and **4**). In contrast, C(6) is slightly more shielded in **1** and **2** than in the parent, but in **3** and **4** C(6) is much more deshielded. Carbon-2, however, is more deshielded in **1**−**4** than in **5**, but for **3** and **4** C(2) is strongly deshielded relative to C(2) in **1** and **2**. In contrast, C(4) is more shielded in **1**−**4** than in **5**. These shielding differences appear on alternate carbons (2, 4, 6, 8); differences in chemical shifts at carbons 1, 3, 5, and 7 of **1**−**4** are generally small. Interestingly, the carbons of the hexanoic acid chain of **1** are more shielded than the corresponding resonances in ester **2**—signifying possible differences in conformation in the chains. No large shielding differences found in the corresponding acid chain carbons of **3** and **4**.

The geometric structural assignments, particularly the *syn-Z*-configuration of the C(4) exocyclic double bond of the dipyrrinone moiety in **1**−**4** was confirmed by the observation of strong nuclear Overhauser effects (NOEs) in $CDCl_3$ between the lactam and pyrrole NHs, and moderate NOEs between the C(5)−H and the C(3) and C(7) methyls (Figure 4). The orientation of the 6-carbon chain was of considerable interest to us. We observed NOEs in **1** between the hydrogens at C(10) and the methyl at C(8), and between the hydrogens at C(10^1) and

(16) For leading references, see: Chen, Q.; Huggins, M. T.; Lightner, D. A.; Norona, W.; McDonagh, A. F. *J. Am. Chem. Soc.* **1999**, *121*, 9253−9264.
(17) Eichinger, D.; Falk, H. *Monatsh. Chem.* **1987**, *118*, 91−103; 261−271.
(18) Montforts, F.-P.; Schwartz, U. M. *Liebigs Ann. Chem.* **1985**, 1228−1253.
(19) Xie, M.; Lightner, D. A. *Tetrahedron* **1993**, *49*, 2185−2200.
(20) Swann, S.; Oehler, R.; Boswell, R. J. *Organic Syntheses*; Wiley: New York, 1943; Collect. Vol. II, pp 276−277.

Table 1. ^{13}C NMR Chemical Shifts[a] of Semirubin 1 (X = H_2, R = H), Its Methyl Ester 2 (X = H_2, R = CH_3), 10-Oxosemirubin 3 (X = O, R = H), Its Ethyl Ester 4 (X = O, R = CH_2CH_3), and Dipyrrinone 5

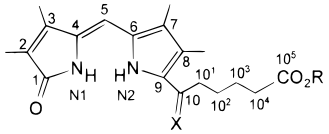

	dipyrrinone chemical shift in $CDCl_3$				
carbon	**1**	**2**	**3**	**4**	**5**
1	174.66	173.89	175.77	173.13	172.3
2	123.58	123.17	134.57	136.76	118.5
3	142.21	142.24	142.72	141.84	141.5
4	128.65	128.34	127.30	128.36	131.6
5	101.29	101.19	98.95	96.80	98.14
6	122.40	122.19	130.50	130.90	124.5
7	125.53	125.22	128.74	129.14	124.1
8	135.81	135.78	125.31	123.52	122.0
9	116.22	115.94	127.89	126.25	120.1
10	22.98	25.68	191.13	189.69	
10^1	21.43	24.82	39.81	39.70	
10^2	26.24	28.68	23.03	23.90	
10^3	28.33	29.89	25.21	24.69	
10^4	32.92	34.02	32.80	34.18	
10^5-CO_2R	180.76	174.21	180.37	173.58	
2-CH_3	8.21	8.63	8.36	8.60	8.57
3-CH_3	9.78	9.93	9.84	9.89	9.36
7-CH_3	9.67	9.71	9.08	9.46	9.83
8-CH_3	8.76	9.06	11.03	11.70	10.26

[a] δ, ppm downfield from $(CH_3)_4Si$ for 10^{-2} M solutions.

the pyrrole NH, indicative of fixed local chain conformation as shown in Figure 4. In contrast, in **2** NOEs are found between the pyrrole NH and both the C(10^1) and C(10) methylenes, and between the latter two and the methyl at C(8)—suggesting a mobile chain conformation. Unlike **2**, but like **1**, NOEs are seen in both **3** and **4** between the pyrrole NH and the C(10^1) methylene, data consistent with a fixed staggered local chain geometry where the C(10) carbonyl is anti to the pyrrole NH, as indicated in Figure 4. A telling NOE was detected between the C(10) hydrogens of **2** (but not **1**) and its methyl at C(2), consistent with the presence of a planar dimer (Figure 2, top). *Significantly, as in bilirubin and mesobilirubin,[11,21] weak NOEs were found between the carboxylic acid hydrogen and the lactam hydrogen in **1** and **3**.* These data indicate a proximal spatial relationship between the carboxylic acid and lactam groups that is consistent with the intramolecular hydrogen bonding motif shown in the structural representation of Figure 3. Although we have no similar information on **4**, it seems likely, given the anti arrangement of its C(10) carbonyl and pyrrole NH, that the ester carbonyl would be in a good position for intramolecular hydrogen bonding to the dipyrrinone NHs. Taken collectively, the NOE data suggest monomeric structures for **1** and **3** (and probably **4**) in $CDCl_3$ solvent and a dimeric structure for **2**.

^{1}H NMR and Hydrogen Bonding. Dipyrrinones are avid participants in hydrogen bonding.[4,9,10] Diagnostic of this behavior and typical of hydrogen bonding pattern in the planar dimer motif (Figure 2), the intrinsic N—H ^{1}H NMR chemical shifts of the monomer (δ ~8 ppm)[9] become strongly deshielded in nonpolar solvents such as $CDCl_3$, to approximately 11 and 10 ppm[9,10,12] for the lactam and pyrrole hydrogens, respectively. However, when the dipyrrinones engage in hydrogen bonding to CO_2H groups to give a stacked dimer (Figure 2, bottom), the NH chemical shifts are relatively more shielded,

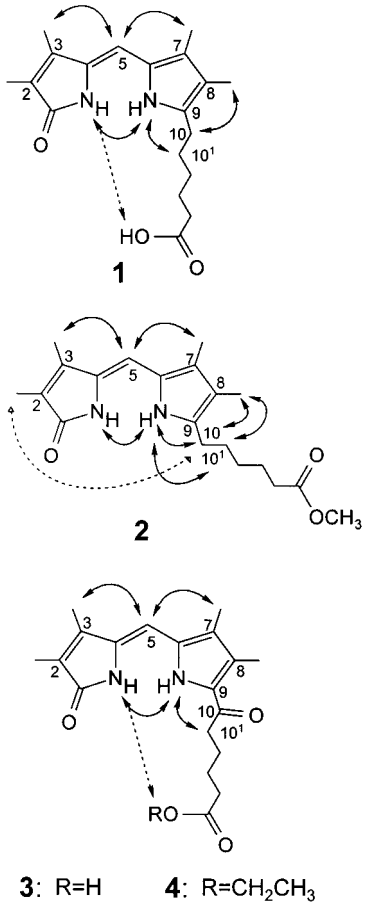

Figure 4. $^1H\{^1H\}$-NOEs found in semirubins **1**—**4** in $CDCl_3$ solvent are indicated by curved double-headed arrows. The dotted arrows signify weak NOEs.

Table 2. Comparison of NH ^{1}H NMR Chemical Shifts[a] of Dipyrrinones in $CDCl_3$ and $(CD_3)_2SO$ Solvents

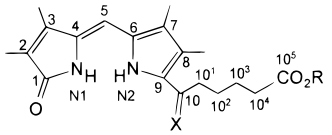

	δ (ppm) in $CDCl_3$[b]			δ (ppm) in $(CD_3)_2SO$[b]		
dipyrrinone	lactam	pyrrole	CO_2H	lactam	pyrrole	CO_2H
1	10.48	8.98	13.22	9.81	10.12	11.95
2	11.17	10.11		9.78	10.12	
3	10.66	9.21	12.80	10.33	10.75	11.99
4	9.14	8.05		10.32	10.74	
5	10.90	10.23		9.7	10.4	

[a] δ, downfield from Me_4Si. [b] Run as 10^{-2} M $(CD_3)_2SO$ and 10^{-3} M $CDCl_3$ solutions at 25 °C.

especially the pyrrole NH (~9 ppm), and to a lesser degree the lactam NH (~10.5 ppm).[10] Similar chemical shifts are also found in tetrapyrroles such as bilirubin, where the dipyrrinones are *intra*molecularly hydrogen bonded to the opposing propionic acids but are not stacked (Figure 1): the lactam and pyrrole chemical shifts lie near δ ~10.6 and 9.2, respectively in $CDCl_3$.[2,7,10] Significantly, the N-*H* chemical shifts of semirubin **1**, notably the shielded pyrrole NH near 9 ppm (Table 2), are similar to those of bilirubin; whereas, those of its methyl ester (**2**) are more like those found in the parent dipyrrinone (**5**). These data thus point to intramolecular hydrogen bonding between dipyrrinone and carboxylic

Table 3. Molecular Weights of Semirubins 1-4 Determined by Vapor Pressure Osmometry[a] at 45 °C in $CHCl_3$ Solution

	molecular weight		
dipyrrinone	calculated	measured by VPO	concentration range (mol/kg)
1	330	337 ± 20[b]	$2.1-6.6 \times 10^{-3}$
2	344	584 ± 30	$1.7-6.1 \times 10^{-3}$
3	344	364 ± 30	$2.2-6.1 \times 10^{-3}$
4	372	373 ± 10	$1.7-5.5 \times 10^{-3}$

[a] Calibrated with benzil (FW = 210, measured MW = 220 ± 15. [b] The VPO study of this compound was initiated in the laboratory of Prof. J. M. Ribó, University Barcelona. Remeasurement in Reno gave the same result.

acid in **1** (Figure 3), and intermolecular dipyrrinone-to-dipyrrinone hydrogen bonding in **2** (as in Figure 2, top). In $(CD_3)_2SO$ solvent, the N-*H* chemical shifts of **1**, **2**, and **5** are all very similar, indicative of hydrogen bonding to the solvent.

Similarly, for oxo-semirubin **3**, the dipyrrinone N-*H* chemical shifts in $CDCl_3$ at ~10.7 and 9.2 for the lactam and pyrrole NHs are indicative of intramolecular hydrogen bonding. Although the presence of a carbonyl group at C(10) can be expected to cause some differences in NH chemical shifts in **3** (and **4**) relative to those of **1**, the shielding of the pyrrole NH in **3** is typical of a dipyrrinone hydrogen bonded to a carboxylic acid. This is accommodated by a structure like that found in ridge-tile bilirubin (Figure 1) and thus on the basis of these data, it seems probable that semirubin and its 10-oxo analogue fold into the conformation shown in Figure 3.

In contrast, the NH chemical shifts of **4** are unusual. Its pyrrole and lactam NH chemical shifts lie at 9.14 and 8.05 ppm, respectively; whereas, in methyl ester **2**, the corresponding chemical shifts lie at 11.17 and 10.11 ppm. While the data for **2** are consistent with an intermolecularly hydrogen bonded dimer, the data for **4** are not, which is perhaps surprising. They are more consistent with intramolecular (or no) hydrogen bonding, which is unusual in dipyrrinone esters. In particular, greater shielding of the pyrrole N-*H* chemical shift of **4** (8.05 ppm) relative to that (9.2 ppm) of intramolecularly hydrogen-bonded **3** is consistent with the absence of hydrogen bonding in **4** and an anti orientation of its C(10) carbonyl relative to the pyrrole NH. One may find a parallel for the dependence of the NH chemical shift on the orientation of the ketone carbonyl group in certain pyrryl ketones. For example, where the carbonyl is syn to the pyrrole NH, as in *tert*-butyl 2-pyrryl ketone the NH chemical shift is 9.5 ppm, but where the carbonyl group is anti, as in *tert*-butyl 2-(3,4-dimethyl pyrryl) ketone it is ~1 ppm more shielded, to 8.6 ppm.[22]

Molecularity in Solution. To assess whether **1**−**4** are monomeric in $CHCl_3$ solution, we determined their molecular weights by vapor pressure osmometry (VPO) over a molal concentration range $1.7-6.1 \times 10^{-3}$. The calibration standard was benzil (MW_{calc} = 210, MW_{obs} = 220 ± 15), and molecular weights determined for **1**−**4** are summarized in Table 3. These data indicate that semirubin **1** and its oxo analogue **3** are monomeric in $CHCl_3$ solution; whereas, **2**, the methyl ester of **1**, tends strongly toward dimerization. Dimer formation in **2** is not surprising in light of earlier observations that methyl xanthobilirubinate and related dipyrrinones are dimeric in nonpolar solvents.[4,9] Surprisingly, but consistent with the NMR analysis above, the oxo-semirubin ethyl ester **4** is monomeric in $CHCl_3$ solution. This is apparently due to the presence and orientation of the oxo group. In **4** the C═O is probably oriented anti to the pyrrole NH−and in this conformation intermolecular hydrogen bonding is apparently prevented by the alkyl chain oriented syn to the pyrrole NH. Although intramolecular hydrogen bonding between the ester and the dipyrrinone is possible in this orientation, the NMR evidence does not clearly support it, since the lactam and pyrrole NH chemical shifts are significantly more shielded than in **3**.

To explore the possibility of a monomer−dimer equilibrium in **1**−**4** over a wider range of concentration, we examined how well the compounds fit Beers Law over the range 1.5×10^{-3} to ~1.5×10^{-6} M. Not surprisingly, and consistent with the absence of a monomer ⇆ dimer equilibrium, acids **1** and **3** gave excellent linearity for plots of absorbance vs concentration (Figure 5A). In contrast, **2** did not match well to the Beers Law prediction (Figure 5B), as might be expected from a monomer ⇆ dimer equilibrium. Contrary to the behavior of ester **2**, oxo-semirubin ester **4** gave nice linearity, indicating that it does not form dimers or other aggregates over the range of concentrations studied. This behavior is unprecedented among simple C-alkylated dipyrrinones or dipyrinone esters, such as methyl xanthobilirubinate.

Molecular Dynamics Calculations. In support of the conclusions reached (above) by NMR spectroscopic analysis, molecular dynamics calculations[23] of semirubin (**1**) and its oxo analogue (**3**) show that these compounds prefer intramolecularly hydrogen-bonded conformations (Figure 6), which are computed to lie some 11.4−12.6 kcal/mol lower in energy than the non-hydrogen-bonded forms. The intramolecularly hydrogen-bonded conformations shown in Figure 6 have computed molecular parameters similar to those found in the dipyrrinones of bilirubin and mesobilirubin.[2,16,24] The dipyrrinone moiety in **1** and **3** is twisted somewhat, with C(4)−C(5)−C(6)−N torsion angles of ~11° and ~22°, respectively. The $C(10^1)-C(10)-C(9)-N$ torsion angles are 66° and 20° in **1** and **3**, respectively − as compared to ~60° in mesobilirubin.[2] While molecular dynamics calculations suggest that **1** adopts a molecular geometry very similar to that found in bilirubin,[2,7,25] the energetically most favored structure of **3** differs somewhat from that of **1**, presumably because its C(10) carbon is sp^2 hybridized rather

(21) (a) Dörner, T.; Knipp, B.; Lightner, D. A. *Tetrahedron* **1997**, *53*, 2697−2716. (b) Nogales, D.; Lightner, D. A. *J. Biol. Chem.* **1995**, *270*, 73−77.

(22) Huggins, M. T.; Tipton, A. K.; Chen, Q.; Lightner, D. A. *Monatsh. Chem.* **2000**, in press.

(23) Molecular Mechanics calculations and molecular modeling was carried out on an SGI Octane workstation using version 6.4 of Sybyl (Tripos Assoc., St. Louis, MO) as described in ref 2. The ball-and-stick drawings were created from the atomic coordinates of the molecular dynamics structures using Müller and Falk's "Ball and Stick" program for the Macintosh.

(24) (a) Falk, H. Molecular Structure of Bile Pigments. In *Bilirubin*; Heirwegh, K. P. M., Brown, S. B., Eds.; CRC Press: Boca Raton, FL, 1982; Vols. 1 and 2, pp 7−29 and references therein. (b) Shelver, W. H.; Rosenberg, H.; Shelver, W. H. *Intl. J. Quantum Chem.* **1992**, *44*, 141−163. (c) Shelver, W. L.; Rosenberg, H.; Shelver, W. H. *J. Mol. Struct.* **1994**, *312*, 1−9.

(25) (a) Bonnett, R.; Davies, J. E.; Hursthouse, M. B.; Sheldrick, G. M. *Proc. R. Soc. London, Ser. B* **1978**, *202*, 249−268. (b) LeBas, G.; Allegret, A.; Mauguen, Y.; DeRango, C.; Bailly, M. *Acta Crystallogr., Sect. B* **1980**, *B36*, 3007−3011. (c) Becker, W.; Sheldrick, W. S. *Acta Crystallogr., Sect. B*, **1978**, *B34*, 1298−1304. (d) Mugnoli, A.; Manitto, P.; Monti, D. *Acta Crystallogr., Sect. C* **1983**, *38*, 1287−1291.

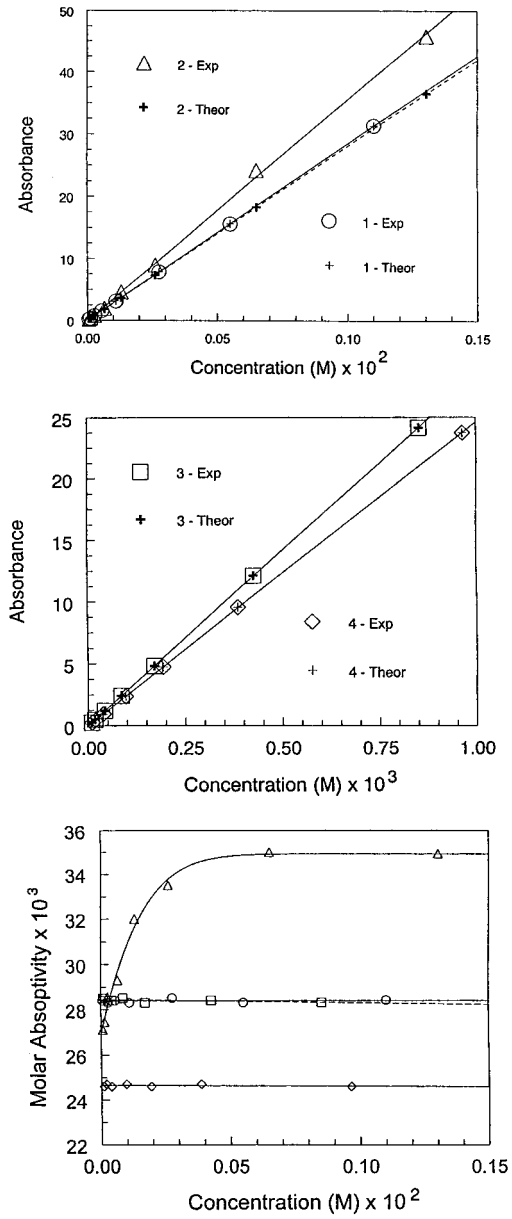

Figure 5. Beers Law plots of absorbance vs concentration in $CHCl_3$ for (A) semirubin **1** (○, +) and semirubin methyl ester **2** (△, +), (B) oxo-semirubin **3** (□, +) and oxo-semirubin ethyl ester **4** (◇, +). Experimental points (○, △, □, ◇); theoretical points (+). (C) Plots of molar absorptivity coefficients (ϵ) vs concentration for **1**−**4** showing linear behavior for **1**, **3**, and **4** but not for **2**.

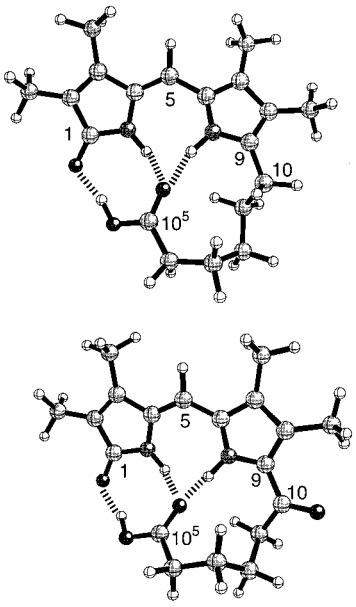

Figure 6. Ball and stick models of the energy-minimized intramolecularly hydrogen-bonded conformations of semirubin **1** (upper) and 10-oxosemirubin **3** (lower). Hydrogen bonds are shown by dashed lines.

than sp^3. Molecular dynamics calculations also indicate a preference (~4 kcal/mol) for an intramolecularly hydrogen-bonded ester carbonyl in **4**, with an overall geometry similar to that of **3**.

Optical Spectra. The UV−vis spectral data for **1**−**4** in solvents with a wide range of polarity are shown in Table 4. The long wavelength bands of semirubin (**1**) and its methyl ester (**2**) have nearly the same λ_{max} in polar solvents, but λ_{max} of **1** is strongly bathochromically shifted from that of **2** in nonpolar solvents, solvents likely to promote hydrogen bonding. Smaller wavelength shifts attend the spectra of oxo-semirubin **3** and its ethyl ester (**4**) over the range of solvents used. While the spectral shifts do not unambiguously confirm an intramolecularly hydrogen bonded structure for **1** and **3**, they lend support to this conclusion, based on NMR spectral analysis and VPO studies, and they are consistent with the ability of **1** and **3** to adopt a unique conformational structure in nonpolar solvents. The UV−vis spectral data for ester **4** are less solvent dependent than those of ester **2**, consistent with the indications that **2** tends toward dimeric in nonpolar solvents and **4** does not.

Solution and Chromatographic Properties. Generally, acids are more polar than esters and thus exhibit smaller R_f values on TLC, as found for xanthobilirubic acid and methyl xanthobilirubinate (Table 5). Such a difference in polarity is less evident in reverse phase HPLC when neither the CO_2H nor the CO_2CH_3 group is involved in intramolecular hydrogen bonding. On the other hand, when the carboxyl group is involved in intramolecular hydrogen bonding, as in bilirubin, the acid typically has a longer retention time than its methyl ester. Although semirubin **1** is more polar than bilirubin, like bilirubin it is insoluble in dilute aqueous bicarbonate. Consistent with these properties, **1** has a shorter retention time (~5.7 min) on reverse-phase HPLC than mesobilirubin-XIIIα (~16.5 min). Semirubin also has a longer retention time than its methyl ester (**2**) (~4.8 min), suggesting that the ester is more polar than the acid. This unusual HPLC behavior (ester more polar than the parent acid) parallels that observed for bilirubin and mesobilirubin-XIIIα and their dimethyl esters and is yet a further indication of intramolecular hydrogen bonding in **1**. However, such clear distinctions in HPLC behavior are less evident for the 10-oxo-semirubin (**3**) and its ethyl ester (**4**), which have similar retention times (~4.0 and ~4.4 min, respectively).

On silica gel TLC, **1** and **3** travel more rapidly than xanthobilirubic acid, consistent with reduced polarity due to intramolecular hydrogen bonding. Dipyrrinone **1** and its methyl ester **2** have nearly the same R_f; whereas, **3** runs faster than its methyl ester. Whether **2** moves unusually fast or **4** unusually slowly is unclear, but the data suggest more effective intramolecular hydrogen bonding in **3** than in **4**. Taken collectively, the chromatographic behavior of **1** and **3** is consistent with a structure

Table 4. Solvent Dependence of UV−Vis Data for Semirubin 1, Oxosemirubin 3 and Their Esters, and Parent Dipyrrinone 5[a]

		λ_{max} (ϵ_{max})[b] for				
solvent	ϵ[c]	**1**	**2**	**3**	**4**	**5**
C_6H_6	2.3	426 (27 300)	411 (33 200)	421 (19 200) 400 (20 600)	415 (16 700) 395 (22 900)	392 (23 500)
$CHCl_3$	4.7	421 (28 400)	407 (28 800)	421 (27 500) 400 (28 600)	415 (19 100) 394 (24 200)	394 (25 300)
CH_3OH	32.6	416 (38 000)	415 (33 500)	411 (22 200) 393 (27 200)	412 (22 100) 393 (26 600)	396 (27 200)
CH_3CN	36.2	411 (25 700)	413 (33 600)	408 (16 300) 386 (21 700)	406 (18 300) 384 (24 000)	395 (26 700)
$(CD_3)_2SO$	49.0	413 (28 000)	411 (33 200)	413 (17 800) 400 (20 600)	414 (16 700) 395 (22 900)	395 (26 300)

[a] Data obtained at 22 °C on $2-4 \times 10^{-5}$ M solutions. [b] λ_{max} in nm, ϵ_{max} in M^{-1} cm^{-1}. [c] Dielectric constants from Gordon, A. J.; Ford, R. A. *The Chemist's Companion*; Wiley: New York, 1972; pp 4−8.

Table 5. HPLC Retention Time and TLC R_f Values for Semirubin Analogues

dipyrrinone	HPLC t_R (min)	TLC R_f[a]
1	5.7	0.45
2	4.8	0.44
3	4.0	0.44
4	4.4	0.26
xanthobilirubic acid	4.2	0.15
methyl xanthobilirubinate	4.1	0.38

[a] In 3% MeOH/CH_2Cl_2 (v/v).

where the polar dipyrrinone and carboxylic acid groups are linked by intramolecular hydrogen bonds (Figure 5). The oxo ester (**4**) data suggest less effective intramolecular hydrogen bonding of its CO_2Et group, whereas semirubin ester **2** is not intramolecularly hydrogen bonded.

Conclusions

Semirubin (**1**), a simple model for one-half bilirubin, has been synthesized and, like bilirubin, is found to adopt an intramolecularly hydrogen-bonded conformation as its energy-minimum structure. As such, it is less polar than its methyl ester and much less polar than bilirubin analogues, e.g., xanthobilirubic acid, that are incapable of intramolecular hydrogen bonding. Similarly, a 10-oxo-semirubin (**3**), a model for 10-oxo-bilirubin, was prepared and found to engage in intramolecular hydrogen bonding. Whether **1** behaves similarly to bilirubin in hepatic metabolism, requiring glucuronidation of its hydrogen-bonded carboxylic acid in order to be excreted into bile, remains to be investigated.

Experimental Section

General Methods. All UV−vis, infrared (IR) spectra and nuclear magnetic resonance (NMR) spectra were determined as reported previously.[7,12] NMR spectra including HMQC, HMBC and NOE experiments were obtained at 500 MHz. Vapor Pressure Osmometry (VPO) measurements were performed in $CHCl_3$ at 45 °C with benzil used for calibration. HPLC analyses were carried out on a Beckman-Altex ultrasphere-IP 5 μm C(18) ODS column (25 × 0.46 cm) and ODS precolumn (4.5 × 0.46 cm). The flow rate was 1.0 mL/min, and the elution solvent was 0.1 M di-*n*-octylamine acetate in 5% aqueous methanol (pH 7.7, 31 °C). Analytical thin-layer chromatography was carried on J. T. Baker silica gel IB-F plates (125 μ layers). Flash column chromatography was carried out using Woelm silica gel F, thin-layer chromatography grade. Radial chromatography was carried out on Merck Silica Gel PF_{254} with gypsum (preparative layer grade). Combustion analyses were carried out by Desert Analytics, Tucson, AZ. Spectral data were obtained in spectral grade solvents (Aldrich or Fisher). All solvents were reagent grade obtained from Aldrich, Acros Organics or Fisher. Deuterated chloroform and dimethyl sulfoxide were from Cambridge Isotope Laboratories. Sodium borohydride, thionyl chloride, aluminum chloride (anhyd), 2-propanol were from Fisher-Acros; hydrochloric acid and glacial acetic acid were from EM Science, Inc; stannic chloride was from J. T. Baker Co.

5-Carbethoxypentanoyl chloride (**6**) was prepared from 5-carboethoxypentanoic acid[20] by standard methods, and 2,3,7,8-tetramethyldipyrrinone[15a,18,19] (**5**) was prepared according to literature procedures.

(4*Z*)-9-(5-Carbethoxypentanoyl)-2,3,7,8-tetramethyl-(10*H*)-dipyrrin-1-one (4). 3,4,7,8-Tetramethyl dipyrrinone (**5**) (0.500 g, 2.3 mmol) and 100 mL of dichloromethane were added to a 500 mL round-bottom flask equipped for magnetic stirring. The solution was cooled in an ice bath for 20 min with stirring; then a solution of acid chloride (**6**) (0.9 g, 4.7 mmol) and $AlCl_3$ (4.5 g, 31.7 mmol) in 100 mL of dichloromethane was added in one portion. The reaction mixture was stirred for 1.5 h at room temperature then poured into a mixture of concentrated HCl (200 mL) and 100 g of ice and stirred for 2 h. The organic layer was separated and the aqueous layer extracted with dichloromethane. The combined organic extracts were washed with saturated aqueous $NaHCO_3$ then with water, and dried over anhydr. Na_2SO_4. The solvent was removed (rotovap), and the crude product was purified by radial chromatography (97:3 by vol. CH_2Cl_2/CH_3OH) and recrystallized from CH_2Cl_2/hexane to afford 0.551 g, 64% of **4**: mp 144−145 °C; IR (KBr) ν 3461, 1737 cm^{-1}; ^1H NMR (DMSO-d_6) δ 1.16 (t, J = 7.5 Hz, 3H), 1.59 (m, 4H), 1.79 (s, 3H), 2.01 (s, 3H), 2.07 (s, 3H) 2.22 (s, 3H), 2.32 (t, J = 6.5 Hz, 2H), 2.82 (t, J = 7.5 Hz, 2H), 5.95 (s, 1H), 10.32 (s, 1H), 10.74 (s, 1H) ppm; ^1H NMR ($CDCl_3$) δ 1.25 (t, J = 7.5 Hz, 3H), 1.74 (m, 4H), 1.93 (s, 3H), 2.06 (s, 3H), 2.10 (s, 3H), 2.30 (s, 3H), 2.35 (t, J = 7.0 Hz, 2H), 2.80 (t, J = 7.5 Hz, 2H), 5.92 (s, 1H), 8.05 (s, 1H), 9.14 (s, 1H) ppm; ^{13}C NMR data are in Table 1 and UV−vis data are in Table 4.

Anal. Calcd for $C_{21}H_{28}N_2O_4$ (372.2): C, 67.70; H, 7.58; N, 7.52. Found: C, 67.69; H, 7.51; N, 7.52.

(4*Z*)-9-(5-Carboxypentyl)-2,3,7,8-tetramethyl-(10*H*)-dipyrrin-1-one (1). Dipyrrinone **4** (275 mg, 0.74 mmol) and 100 mL of 2-propanol were placed in a 250 mL round-bottom flask equipped for magnetic stirring. Sodium borohydride (100 mg, 1.7 mmol) was added, and the reaction mixture was heated at reflux for 2 h. The hot reaction mixture was poured into 100 mL of ice water, and the solution was acidified with 10% aq. HCl. The suspension was extracted with dichloromethane, and the combined organic extracts were washed with water and dried over Na_2SO_4 (anhydr.). The solvent was removed (rotovap), and the crude product was purified by radial chromatography (97:3 by vol. CH_2Cl_2/CH_3OH) and recrystallized from CH_2Cl_2/hexane to give 0.215 g of **1**, 88% yield: mp 210−211 °C; IR (KBr) ν 3347, 1707, 1654 cm^{-1}; ^1H NMR ($CDCl_3$) δ 1.42 (m, 2H), 1.60 (m, 2H), 1.74 (m, 2H), 1.92 (s, 3H), 1.96 (s, 3H), 2.11 (s, 3H), 2.13 (s, 3H), 2.52 (t, J = 5.5 Hz, 2H), 2.75 (t, J = 6.0 Hz, 2H), 6.13 (s, 1H), 8.98 (s, 1H), 10.48 (s, 1H), 13.22 (s, 1H) ppm; ^1H NMR (DMSO-d_6) δ 1.29 (m, 2H), 1.52 (m, 4H), 1.77 (s, 3H), 1.86 (s, 3H), 2.00 (s, 3H), 2.06 (s,

3H), 2.20 (t, $J = 8.0$ Hz, 2H), 2.50 (t, $J = 7.5$ Hz, 2H), 5.93 (s, 1H), 9.81 (s, 1H), 10.12 (s, 1H), 11.95 (s, 1H) ppm; ^{13}C NMR data are in Table 1 and UV−vis data are in Table 4.

Anal. Calcd for $C_{19}H_{26}N_2O_3$ (330.2): C, 65.86; H, 7.57; N, 8.29. Calcd for $C_{19}H_{26}N_2O_3 \cdot {}^1/_2H_2O$ (339.2): C, 67.20; H, 8.02; N, 8.26. Found: C, 66.80; H, 7.86; N, 8.48.

(4*Z*)-9-(5-Carbomethoxypentyl)-2,3,7,8-tetramethyl-(10*H*)-dipyrrin-1-one (2). Semirubin **1** (68 mg, 0.20 mmol) and 50 mL of methanol were added to a 100 mL round-bottom flask equipped for magnetic stirring. Ten milliliters of 10% aq. H_2SO_4 were added to the solution dropwise over 5 min, and the reaction mixture was heated at reflux for 1 h. The reaction mixture was cooled to room temperature, taken up in dichloromethane, and washed with and saturated aq. sodium bicarbonate solution. The organic extract was dried over Na_2SO_4 (anhydr) and the solvent removed (rotovap). The residue was purified by radial chromatography (97:3 by vol. CH_2Cl_2/CH_3OH) and recrystallized from CH_2Cl_2/hexane to give the desired product, **2**, (65 mg) in 92% yield: mp 187−188 °C; IR (KBr) ν 3348, 1736 cm^{-1}; ^{1}H NMR ($CDCl_3$) δ 1.35 (p, $J = 7.5$ Hz, 2H), 1.65 (m, 4H), 1.95 (s, 3H), 2.00 (s, 3H), 2.11 (s, 3H), 2.13 (s, 3H), 2.29 (t, $J = 8.0$ Hz, 2H), 2.75 (t, $J = 7.5$ Hz, 2H), 3.64 (s, 3H), 6.13 (s, 1H), 10.11 (s, 1H), 11.17 (s, 1H) ppm; ^{1}H NMR (DMSO-d_6) δ 1.27 (m, 2H), 1.53 (m, 4H), 1.76 (s, 3H), 1.84 (s, 8H), 1.99 (s, 3H), 2.04 (s, 3H), 2.29 (t, $J = 7.0$ Hz, 2H), 2.49 (t, $J = 7.5$ Hz, 2H), 3.56 (s, 3H), 5.91 (s, 1H), 9.78 (s, 1H), 10.11 (s, 1H) ppm; ^{13}C NMR data are in Table 1 and UV−vis data are in Table 4.

Anal. Calcd for $C_{20}H_{28}N_2O_3$ (344.2): C, 69.72; H, 8.20; N, 8.14. Found: C, 69.79; H, 8.30; N, 8.18.

(4Z)-9-(5-Carboxypentanoyl)-2,3,7,8-tetramethyl-(10*H*)-dipyrrin-1-one (3). Dipyrrinone (**4**) (77 mg, mmol) and 50 mL of tetrahydrofuran were placed in a 100 mL round-bottom flask equipped for magnetic stirring. Ten milliliters of 2 M NaOH (aq) were added, and the reaction mixture was heated at reflux for 3 h. The hot reaction mixture was poured into ice−water and acidified with 10% aqueous HCl. The suspension was extracted into dichloromethane and washed with water. The combined organic extracts were dried over anhyd. sodium sulfate and evaporated (rotovap). The residue was purified by radial chromatography (97:3 by vol. CH_2Cl_2/CH_3OH) and recrystallized from CH_2Cl_2/hexane. Pure acid **3** (64 mg) was obtained in 90% yield: mp 197−198 °C; IR (KBr) ν 3374, 1698 cm^{-1}; ^{1}H NMR (DMSO-d_6) δ 1.59 (m, 4H), 1.80 (s, 3H), 2.02 (s, 3H), 2.08 (s, 3H), 2.23 (s, 3H), 2.25 (t, $J = 6.5$ Hz, 2H), 2.83 (t, $J = 7.0$ Hz, 2H), 5.96 (s, 1H), 10.33 (s, 1H), 10.75 (s, 1H), 11.99 (s, 1H); ^{1}H NMR ($CDCl_3$) δ 1.83 (p, $7J = .0$ Hz, 2H), 1.95 (p, $J = 7.0$ Hz, 2H), 1.95 (s, 3H), 2.11 (s, 3H), 2.15 (s, 3H), 2.35 (s, 3H), 2.56 (t, $J = 7.0$ Hz, 2H), 2.88 (t, $J = 7.0$ Hz, 2H), 6.09 (s, 1H), 9.21 (s, 1H), 10.66 (s, 1H), 12.80 (s, 1H); ^{13}C NMR data are in Table 1 and UV−vis data are in Table 4.

Anal. Calcd for $C_{19}H_{24}N_2O_4$ (344.2): C, 66.25; H, 7.03; N, 8.14. Found: C, 65.98; H, 6.87; N, 7.98.

Acknowledgment. We thank the National Institutes of Health (HD-17779) for support of this research. We are grateful to Prof. Josep M. Ribó (Departament de Química Orgànica, Universitat de Barcelona) for the initial VPO studies of compound **1**. We are indebted to Prof. Thomas W. Bell of this department for allowing us to use the vapor pressure osmometer. M.T.H. is an R. C. Fuson Graduate Fellowship awardee.

Supporting Information Available: NMR spectra for compounds **1**−**4** in $CDCl_3$ solvent are reported herein. This material is available free of charge via the Internet at http://pubs.acs.org.

JO000393K